Considerations for qualifying reliable eddy current array technique for detection of backwall cracks

Ajay M. Koshti, NASA Johnson Space Center, Houston, U. S. A.

ABSTRACT

A reliable nondestructive evaluation (NDE) technique provides minimum 90% probability of detection (POD) with 95% confidence for detection of cracklike flaws of a qualified size. In this case, the flaws are on backside of material. Eddy current array (ECA) probe or a single sensor eddy current probe in c-scanning mode is used for the flaw detection. Here, two geometries are considered for the test specimens. The two geometries are, a flat plate, and tube or pipe. The probe is assumed to be on outer diameter (OD) surface and the flaw is assumed to be at the inner diameter (ID) surface for tube inspection. The flaw and probe are on opposite side of wall thickness for inspection of plate material. The application may be used for acreage inspection or just for inspection of butt weld and heat affected zone (HAZ) in a tube, cylinder, or plate. The proposed approach is based on developing an instrument standardization or calibration procedure. Decision threshold of inspection procedure is determined using empirical qualification and noise data. The work explores essential parameters that are required to meet certain conditions to ensure reliable flaw detection. Physics-based simulation of eddy current array flaw detection is used to understand effect of essential parameters on signal response (amplitude and phase), and therefore flaw detectability. Simulation data is used to justify choice of calibration reference standard requirements and the qualification approach. An ECA technique qualification model is provided. The paper gives brief description of tasks to be completed for qualifying ECA technique for reliable detection of cracklike flaws.

Keywords: Eddy current array inspection, nondestructive evaluation, qualification, reliability

1. INTRODUCTION

A number of suppliers including Eddyfi Technologies[1], SG NDT[2], Evident/Olympus[3], Zetec[4] Inc. and Uniwest[5] provide eddy current array (ECA) equipment. Some of these suppliers also provide single sensor eddy current probes and instruments. ECA testing has some advantages over the single sensor eddy current testing. Array has a larger footprint i.e., the effective probe length within which flaws are detected is much larger. Therefore, a single scan-pass covers much larger area compared to a single pass of the single sensor probe. ECA testing provides real time inspection data map or C-scan corresponding to inspection surface. Inspection data map facilitates flaw detection and data interpretation. ECA scanning simplifies complexity of scanning compared to single sensor which uses raster scanning. ECA scanning is much faster compared to single sensor scanning. If ECA inspection is properly qualified, it would provide an alternate reliable crack detection technique to other techniques such as x-ray radiography and ultrasonic testing.

The eddy current application is either to inspect plain material or a butt weld joint with adjacent heat affected zone (HAZ). The inspection is termed as volumetric, as backwall surface, embedded and front (probe-side) wall surface flaws are to be detected. In case of a weld, there may be a weld reinforcement or additional material compared to parent wall thickness in crown and/or in root region. The inspection assumes that walls of the two tubes that are joined in butt weld have same material, diameter, and wall thickness providing a more-or-less constant weld cross sectional geometry. Constant wall thickness is assumed for the parent material of the plate. Uniform electrical conductivity and relative magnetic permeability of 1 are assumed in the inspection region. It is assumed that ECA probe conforms to contact surface including the weld OD surface. Weld surface textures/topography would cause some probe lift-off locally at low points of the texture. Effect of varying lift-off should be accounted for in the procedure qualification, calibration, and actual inspection. Normally, the probe scans the circumferential weld of a tube in a circumferential direction to cover the entire tube weld in one 360° circumferential pass. A small variation in electrical conductivity and permeability may be tolerated as long as the material property does not vary a lot in circumferential direction which is the scan direction for the ECA probe. The signal variation effects should also be accounted for in the procedure qualification testing. This discussion is equally applicable to the single sensor EC inspection.

Although, the objective is stated as detecting backwall flaws reliably, it can be further modified as detecting embedded flaws of certain size throughout the wall thickness reliably. The worst-case embedded flaw location within the wall thickness may provide slightly smaller signal response than the same size flaw at the backwall. The flaw geometries of interest are given in NASGRO[6]. The backwall surface flaws are assumed to have a semi-elliptical shape. The embedded flaws are assumed have elliptical shape. Depth is denoted by letter "*a*" and length is denoted as "2*c*" for surface flaws. Depth is denoted by "2*a*" and length is denoted by "2*c*" for embedded flaws. Part thickness is denoted by letter "*t*".

Bishop[7] provides qualification data analysis for original Standard NDE which includes surface crack detection using conventional or single sensor eddy current testing. Parker[8] provides updated guidelines for Standard NDE qualification. This work uses CIVA[9] 2023 software eddy current module to suggest approach for qualification of ECA and conventional eddy current for reliable detection of cracklike flaws on backwall of part. The simulation work identifies sensitivities of various input parameters that must be accounted for in empirical ECA qualification. Noise is not accounted for in CIVA simulation. LS-POD[10] and NDE transfer functions[11-13] are applicable for the empirical work in ECA technique qualification. Contrast-to-nose ratio[14-15] (CNR) based flaw detection is also applicable for this work which accounts for multiple pixels within the flaw indication.

This work recommends a number of tasks towards qualifying an eddy current technique. These are: development of written procedure, development of instrument standardization (calibration), estimation of transfer function or ratios between calibration flaw response and the assumed induced natural flaw in part, part noise analysis, determining decision threshold to requirements set in the written procedure, verifying that the ECA procedure meets the flaw detection reliability requirements, designing POD testing protocol, POD testing by operators, POD analysis and qualification/certification reports and documentation. If reliability requirements given in the Standard ECA procedure or those given in the Special ECA certification are met, then ECA procedure is assumed to provide 90/95% POD/Conf. in detection of the qualified size flaw.

2. FLAW ORIENTATIONS AND ECA PROBE TOPOLOGY

All flaw planes are assumed to be normal to the OD or ID surface. Three angular flaw orientations are of interest. These orientations are axial (0°), transverse (90°), and 45° between transverse and axial orientations. See Fig. 1. A typical ECA probe has many transmit/receive coil configurations or topologies. Within a given topology there may be axial and transverse modes. A coil that is energized is referred to as transmit (T) coil. While sensing coil is referred to as receiving (R) coil. The ECA probe is normally scanned in a direction normal to coil row or length direction. This is called the scan axis. See Fig. 1. The axial topology is sensitive to detection of axially oriented or scan axis-oriented flaws. The transverse topology is sensitive to detection of transversely oriented flaws. Examples of specific axial and transverse topology are given in Fig. 1. Both topologies are less sensitive to detection of a flaw oriented at 45° to axial or circumferential direction. Thus, 45° orientation is considered to be the worst-case among the three orientations for axial and transverse coil topologies. There is another topology called transmit/receive (T/R). There are two modes of T/R topology. These are absolute and differential. In absolute T/R topology, each coil does both energizing and sensing independently i.e., when other coils are not energized or sensing. Eddy current field is limited to a single coil at a time and is narrower than some of the axial and transverse topologies. The absolute T/R topology may be less desired for backwall flaw detection due to lower EC field penetration depth compared to the other probe topologies. However, the absolute T/R topology is simpler to program in a simulation software and provides useful information for this work. See Fig. 1. Short topology may be optimal for detection of shallower flaws and long topology may be optimal for detection of deeper flaws. Resolution may be affected by choice of short and long topologies due to change in distance between transmit and receive coils.

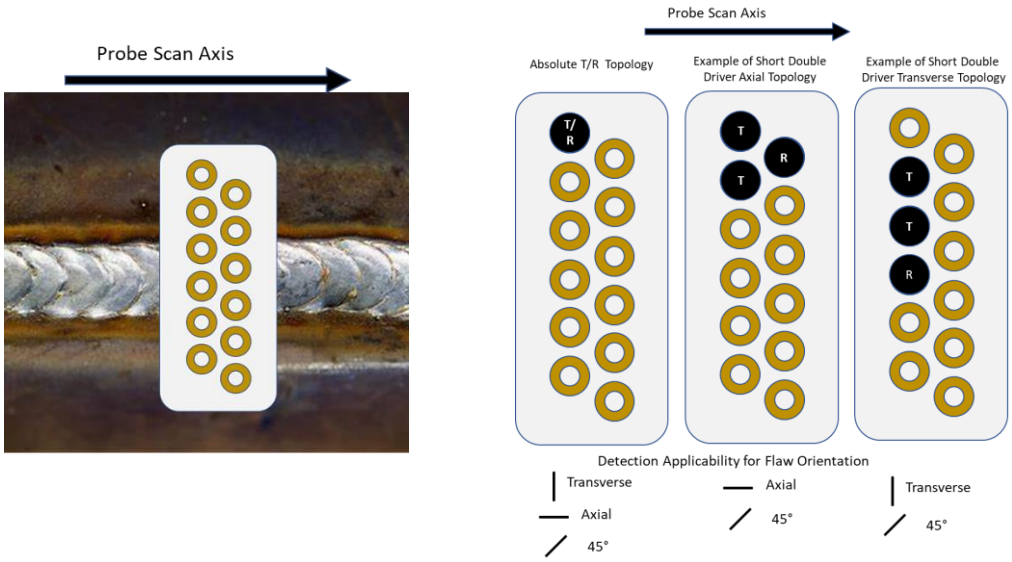

Fig. 1: Array coil topologies

3. RELIABLY DETECTABLE ECA CRACK SIZE AND CONSTRAINTS

Current work is towards qualifying a reliable ECA flaw detection technique. There are two kinds of reliable flaw detection NDE techniques. These are described as Standard and Special. A fixed backwall surface flaw size e.g., $a = 0.7t$, $a/2c = 0.5$, 0.030"$\leq t \leq$ 0.180", and 1 $\leq$ %IACS $\leq$100 may be generically qualified by qualifying technique requirements for Standard ECA technique. In addition to $a/2c = 0.5$ thumbnail flaw, reliable detection of longer flaws e.g., $a/2c = 0.1$ with shorter depths e.g., $a = 0.5t$ may be desired by fracture control. Increase in flaw length increases signal response to a limit based on technique resolution. Shortening depth and increasing length have opposing effects on the signal response. The net effect may provide adequate signal response for reliable flaw detection. The two aspect ratio flaws should be covered as two separate target flaws in the reference standard and qualification testing.

Special eddy current qualification is specific to a selected EC procedure, for inspecting specific parts by an operator who passes the POD demonstration test. The ECA reliably detectable or qualified flaw size will be determined after completion of the qualification tasks. A qualified flaw size and any constrains on material thickness, electrical conductivities would be finalized after the qualification. A qualified flaw size of $a = 0.5t$ with $a/2c = 0.5$ has significant benefit as ECA qualified to this flaw size may provide an alternate method to x-ray inspection for crack detection in butt welds provided process control ensures that volumetric flaws such as porosity, inclusions, and other geometric anomalies do not exceed acceptance criteria limits. A qualified flaw size of $a = 0.5t$ with $a/2c = 0.5$ may also be a reasonable target for qualification testing for Standard ECA inspection of thin wall tubing or pipes. Detection of slightly shallower ($a \leq 0.5t$) backwall flaw may be possible and may be better suited for Special ECA testing procedures due to reduced inspection sensitivity.

ECA standard depth of penetration (DOP) depends upon conductivity and probe frequency. Flaw ligament or distance between the probe contact surface and closest tip of cracklike flaw cannot be more than a few (e.g., 2) times of depth of penetration for backwall flaw detection due to reduced sensitivity. Probe frequency is limited by probe design. ECA probes are available in certain frequency ranges e.g., 100 Hz to 4 MHz. Limit on flaw ligament also implies limit on part thickness. Therefore, in order to define a Standard ECA flaw size at fixed a/t, constraint on DOP/t ratio is justified.

Lower frequency probes have larger coil diameter and resolution distance is larger. Typically, resolution distance is larger for detection of deeper flaws and lower limit on the length of detectable deeper flaws is higher. Moreover, availability of probe designs limit available probe resolution distance r. Cracklike flaws with length smaller than probe resolution distance are not likely to be detected reliably. Therefore, constraint on $2c/r$ ratio is also justified.

4. ECA SIMULATION CONSIDERATIONS

Goal of the physics model-based simulation is to assist in defining qualification tasks. The reference standard design involves making design choices for flaw type, size, location, orientations for both the calibration reference standards and qualification testing specimens. Simulation can provide insight into relative effect of relevant parameters or variables on signal response. Exact input parameters of actual inspection set-ups will not be used in the simulation. If exact input parameters of each inspection set-up are simulated, it will result in many simulation runs as there are multiple ECA techniques; each with specific values for electrical conductivity, wall thickness, flaw dimensions, flaw ligament dimension, flaw gap tightness or contact. Moreover, probe design, probe topology, filtering settings etc. also contribute to combinations of essential input parameters resulting in many set-ups. Despite choosing correct values of all input parameters as much as allowed by the simulation software, there will be differences in simulation signal response and measured signal response. The simulation cannot not model all essential variables ECA inspection to provide accurate prediction of empirical signal response and noise.

Therefore, it is advisable to limit use of simulation for studying relative influence of some of essential input parameters. CIVA NDE 2023 ECA module is used for simulation. Overall noise, which contains electronic noise, material property variation noise, surface topology variation noise, and scanning/lift off variation noise, is not simulated in the software. Some electronic noise is simulated. Therefore, the simulation is not meant to assess probability of detection (POD) and probability of false positive (POF) from this data. Simulation is meant to reveal signal response correlation to some of input parameters that need to be controlled in the ECA technique qualification and inspection. Simulation cannot replace ECA instrument standardization (calibration) and empirical qualification of EDM-to-crack response transfer ratio, and empirical transfer function analysis for POD testing. Reliability of each ECA procedure should be individually verified to meet requirements given in the respective procedure.

Some of the useful simulation studies include studying change in signal response for change in following input parameters or conditions,

1. Flaw depth for backwall flaw
2. Flaw gap electrical contact or filling rate
3. Flaw length
4. Ligament for a fixed a/t and $a/2c$ flaw
5. Frequency and electrical conductivity
6. Flaw geometry from rectangular to semi-elliptical
7. Flaw orientation
8. Probe topology variation i.e., axial, transverse and transmit/receive (T/R)
9. Weld geometry versus constant thickness plate

All above input parameters affect some of the three output quantities related to probability of detection which are signal response (sensitivity), resolution and relative noise. Parameters from 1 through 7 relate to sensitivity. The filling rate or % contact between flaw faces simulates a tight crack with intermittent contact between crack faces. A number from 0 to 100% can be chosen for filling rate to simulate a tight crack. Certain range and distribution (i.e., normal distribution) of filling rate may provide signal response distribution that is close to that from natural cracks of same length, depth, and shape. Product of frequency and conductivity relates to standard depth of penetration (DOP) for non-ferromagnetic parts. Therefore, DOP-to-part thickness ratio will be used to describe frequency and conductivity together. Parameters 8 through 9 may affect more than one output quantity. Simulation with variation in parameters 8 and 9 will not be covered in this paper. Parameters 8 and 9 can be accounted for empirically for a given ECA application.

Resolution distance is related to center-to-center distance between coils. Multiple staggered rows may provide better resolution than just distance between coils. Resolution is the smallest length of a flaw that can be detected or imaged with 20% modulation transfer function value compared to a much longer flaw. Resolution distance relates to minimum separation distance between two adjacent identical flaws needed to form two separate indications or detections. A number of open flaws (e.g., notches) with same depth but differing length can be used to determine the resolution distance in ECA testing. Here, it is assumed that flaws with length greater than 5 times of the resolution distance provide the same maximum

signal response. Probe coil topology and flaw orientation should be considered for defining resolution. Resolution distance is larger for detection of deeper flaws. Normally, resolution is not measured in ECA testing, however it is an important factor as it relates to smallest flaw length that can be reliably detected in a given ECA inspection set-up.

This paper would consider a simpler case of probe topology to conduct simulation. Only T/R topology is considered as it is less complex for simulation. It is the most basic ECA topology for simulation. Many short and long axial and transverse topologies are possible and are chosen depending upon the ECA application. Longer topologies are useful for detection of deeper flaws. It is assumed that any conclusions using simulation of T/R topology will be equally applicable for other topologies. The calibration procedure should account for 0, 45 and 90° flaw orientations in the chosen probe coil topologies. 45° flaw orientation provides lower signal response compared to axial topology for detecting axial flaw. Similarly, 45° flaw orientation provides lower signal response compared to transverse topology for detecting transverse flaw. Therefore, 45° orientation notch will be used in simulation, as it provides a lower bound on signal response. It is assumed that backwall surface flaw will be necessary to calibrate the backwall flaw detection decision threshold.

Two types of flaws such as rectangular and semi-elliptical will be used in the simulation. A rectangular flaw is useful in conducting parametric study for effect of change in ligament for an embedded flaw with fixed depth. Here, zero value for ligament on ID and OD side is possible. The embedded flaw shape of interest is elliptical for NASGRO[6]. Similarly, surface flaw shape of interest is semi-elliptical with flat side on the surface. Thus, there is a transition in shape from semi-elliptical to elliptical when flaw location changes from surface to embedded. It is difficult to accommodate the flaw shape transition in parametric study of changing ligament length for a given depth flaw. Therefore, rectangular shape flaw will be used for parametric study with ligament change. Elliptical surface flaw responses will be compared with same dimension (length and depth) rectangular flaw in a different simulation run.

5. SIMULATION RUN 1 FOR VARIATION IN FLAW LENGTH, FLAW DEPTH AND FILLING RATE

Fig. 2 gives a schematic of CIVA ECA simulation scan input.

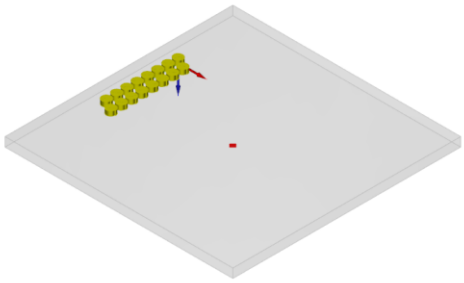

Fig. 2: CIVA 2023 ECA simulation scan input graphics

Here, following input parameters are used.

1. Specimen: Geometry type → Planar, Height → 2 mm, Length→50 mm, Width→50 mm
2. Material: Name → Stainless Steel 304L, Density → 7.8 g.cm-3, Electrical Conductivity → 0.8 MS.m^{-1}, Relative Permeability → 1
3. Probe: Rows of coils → 2, Coils in a row → 8, Coil diameter → 2 mm, Step X → 2.25 mm, Step Y → 2.25 mm, Shift X → 0 mm, Shift Y → 1.25 mm, Coil OD → 2 mm, Coil type → Spiral (Pancake) Coil, Topology → Transmit/receive
4. Scanning: Step → 0.8 mm
5. Flaw: Position → backwall, Type → Rectangular or parallelepiped notch, **Bridge contacts or Filling rate → 0-50%**, Bridge pattern → Random, Flaw width → 0.1 mm, **Flaw length, 2*c* → 1-9 mm**, **flaw depth, *a* →0.6-1.4 mm**, Skew → 45°. Flaw model: VIM (Volumetric Integration Model)
6. Acquisition: Frequency (kHz) → 175, Phase → 90 deg, Current → 0.01mA

7. Standard depth of penetration (DOP)/part thickness t = 0.66
8. Standard depth of penetration (DOP)/ligament = 1.32
9. $\frac{2c}{r} = 0.8 - 7.2$, Assume resolution $r = 1.25$.

Staggered second row of coils in the probe implies resolution would be related to half of the coil spacing. Half of coil spacing is ~1.25 mm. Run 1 is a parametric study of first 3 parameters which are: 1 - flaw depth for backwall flaw, 2 - flaw gap electrical contact, and 3 - flaw length. Fig. 3 shows ECA simulation results for a specific case.

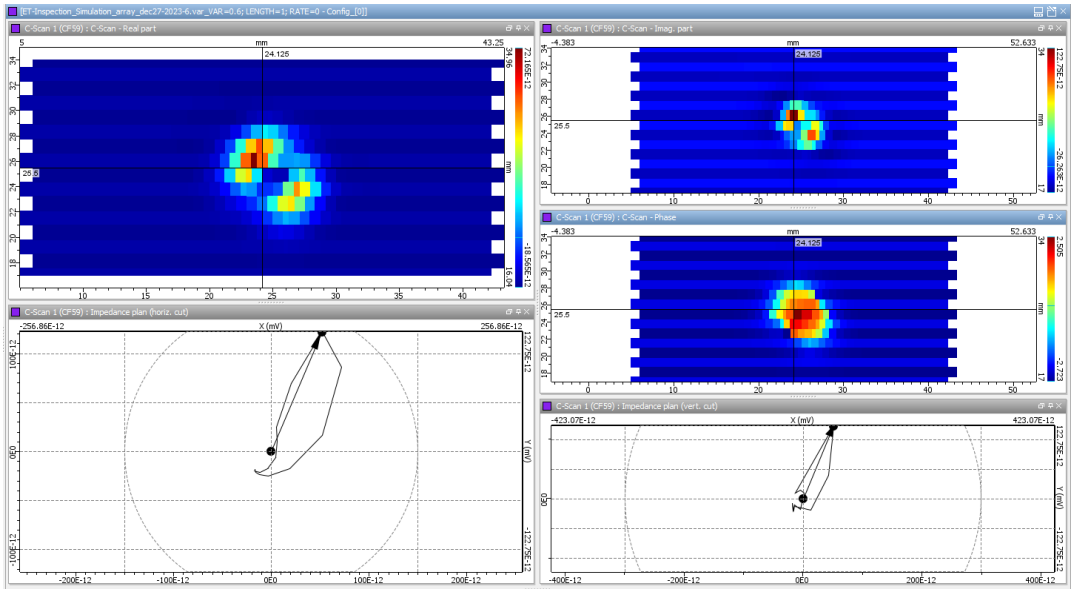

Fig. 3: ECA scans showing real part, imaginary part, and phase. Flaw depth (VAR) = 0.6 mm (a/t = 0.3), length = 1 mm, filling rate = 0%.

Although, the results show image of the flaw, the magnitude is smaller by one order of magnitude compared to (a/t = 0.7) flaw in Fig. 7.

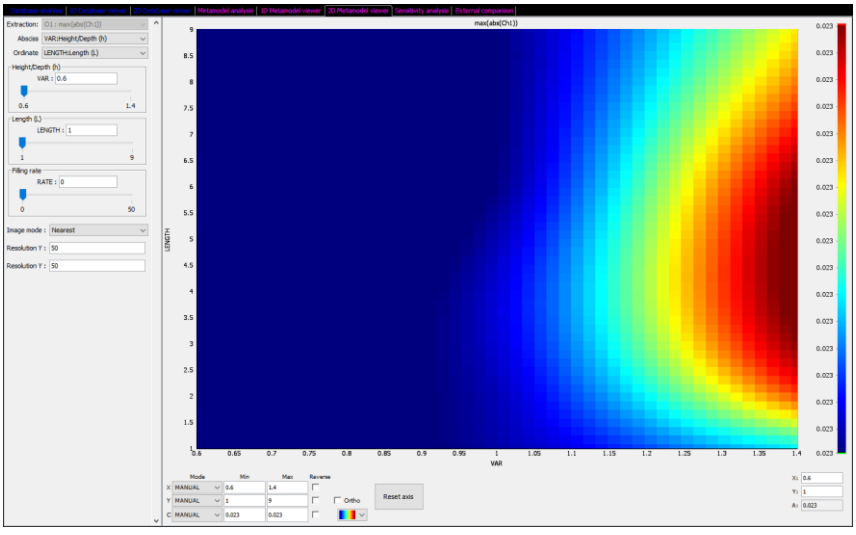

Fig. 4: Results of notch depth, length, and notch filling rate parametric study with open notch (filling rate = 0%). Map of maximum of absolute impedance plane amplitude. VAR = flaw depth. Dimensions in mm

Fig. 4 shows ECA results in detection of a notch. Fig. 4 indicates that flaw depths under 1 mm are not as detectable at any length. Signal response for flaw lengths under 1 mm and under 1.1 mm depth have much lower value compared to the maximum registered at 1.4 mm depth and 4.5 mm length. Based on examining the bottom right point in Fig. 4, resolution seems to be slightly less than 1 mm in the current set-up for detecting 45° oriented flaws. The probe coil rows intersect the 45° oriented long flaw in a fixed shorter length. Therefore, for longer flaws only fixed short length of flaw is under probe field at any one time. Signal response does not increase beyond a limit for longer flaws. Maximum of absolute impedance plane amplitude is displayed. The amplitude has a bias of a constant number ~0.023 units corresponding to the background of the indication. The background value can be subtracted to get relative amplitude.

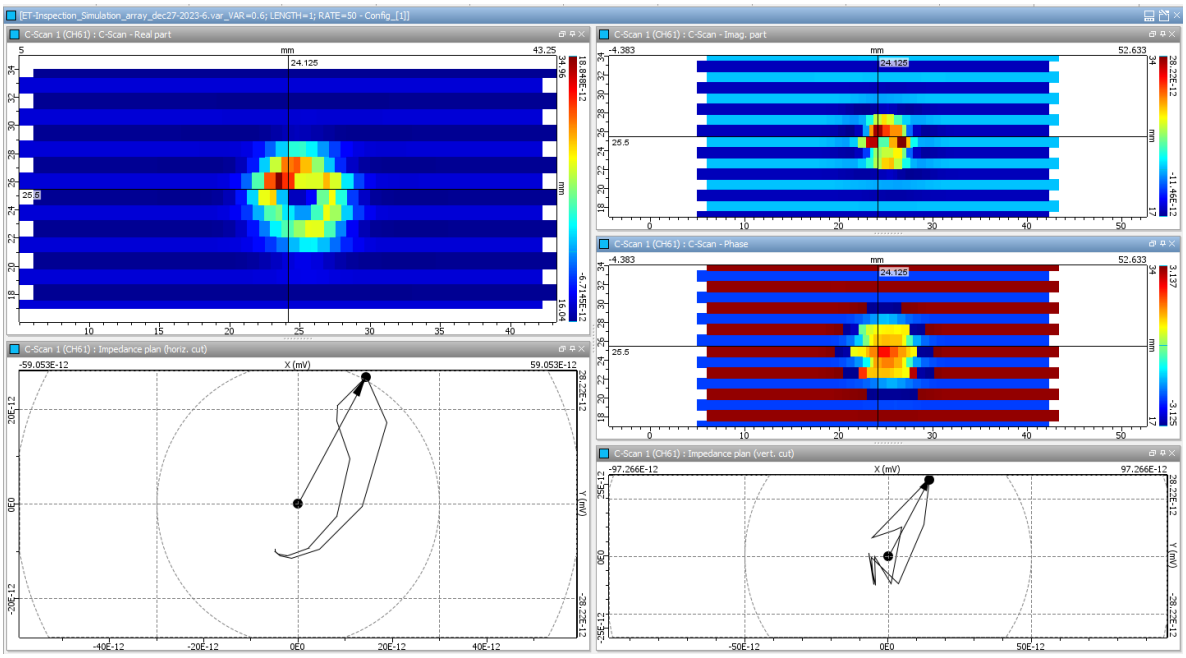

Fig. 5: ECA scan, real part, imaginary part and phase, flaw depth= 0.6 mm, length = 1 mm, filling rate = 50%.

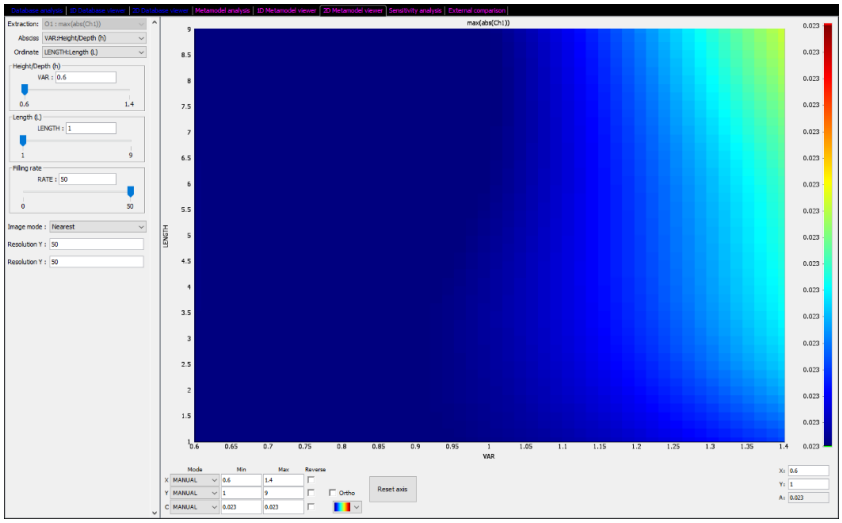

Fig. 6: Results of variation in notch depth, length, and notch filling rate parametric study. Notch filling rate = 50%. Map of maximum of absolute impedance plane amplitude. VAR = flaw depth. Dimensions in mm

Fig. 5 shows ECA results in detection of a tight crack and the relative amplitude values are much lower than those in Fig. 4. Although, the results show image of the flaw, the magnitude is smaller by one order of magnitude compared to filling rate = 0 % flaw in Fig. 3. The filling rate can be chosen between 0 to100% in the simulation. One can determine a filling rate that matches with empirical data i.e., relationship between signal responses of EDM flaw and crack of same size.

Fig. 6 indicates that longer flaws have higher amplitude for flaws with filling rate of 50%.

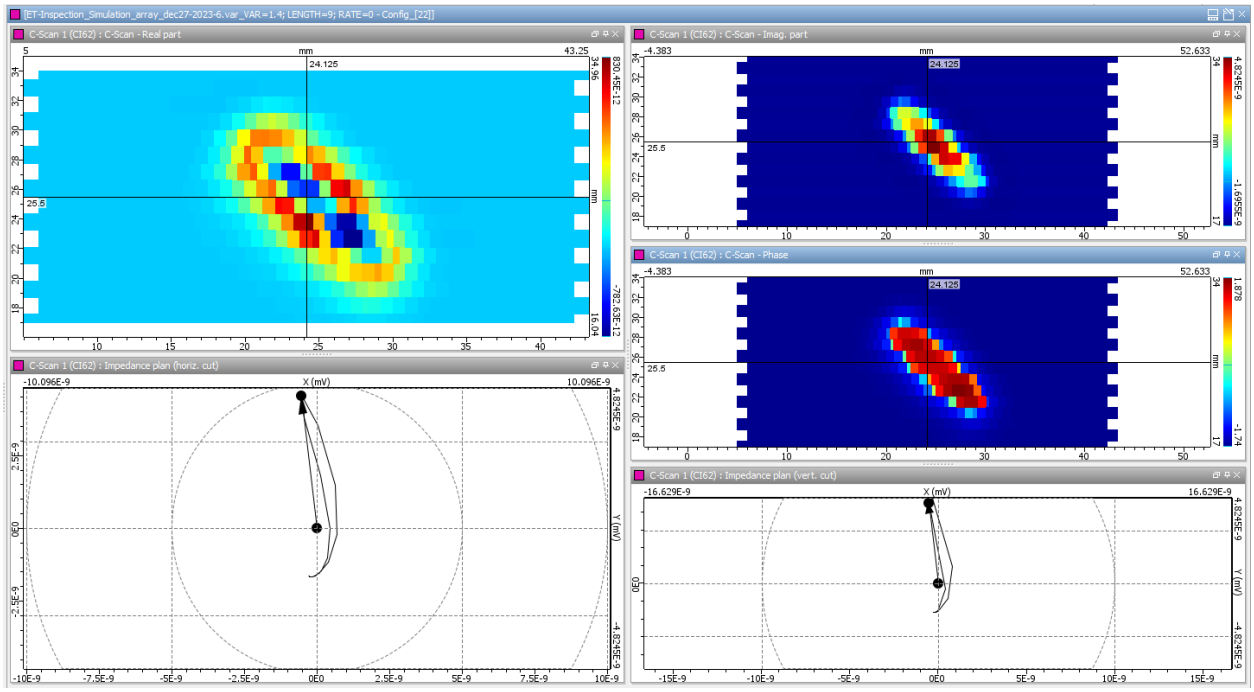

Fig. 7: ECA scan, real and imaginary parts, flaw depth= 1.4 mm, length = 9 mm, filling rate = 0%.

Fig. 4 and 6 give absolute maximum impedance plane signal amplitude. Signal amplitude relative to background (null point) is useful for threshold-based flaw detection. The flaw is imaged as a cluster of pixels. One of the pixels would have a maximum value that would be used in threshold-based detection. However, flaw is also detected visually by detecting the pixel cluster. Visual flaw detection is similar to detection based on contrast-to-noise ratio (CNR)[7]. The longer and deeper flaw indication of Fig. 7 has many more pixels than shallow and short flaw indication of Fig. 3. Therefore, indication in Fig. 7 would be more detectable due to more pixels (counted within the imaginary 6 dB boundary) of the indication. Therefore, using the maximum value of a single pixel for threshold-based flaw detection does not compare with visual detection of flaw indications for very low maximum amplitude or low CNR indications. Visual detection of indication is very important and CNR based detection can provide better match with visual flaw detection. Simulation Run 1 shows following sensitivity analysis.

Based on the analysis, flaw depth is a primary factor affecting signal response followed by filling rate or % contact area in crack faces. Length is the last factor in terms of sensitivity. Flaw depth is at least 30 times more sensitive than the other two factors. Some indications with longer length-to-width aspect ratio (~ 6-8) may be detectable at lower CNR than those at lower aspect ratio[8]. Therefore, length of flaw is also an important factor in visual flaw detection. These results indicate that the calibration notch should have same depth and length to the target flaw size. The flaw face contact filling rate changes the overall amplitude map in terms of amplitude distribution as evident by comparing the Fig. 4, Fig. 6, and Fig. 9. If notch-to-crack amplitude transfer ratio is under 2:1 and overall absolute amplitude distribution looks similar, then simple transfer ratio factor may be applicable for flaws with $2c \geq t$. These limits may be different for different frequency and probe coil topology.

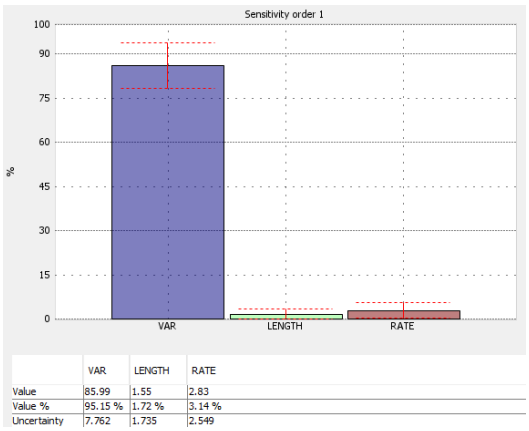

	VAR	LENGTH	RATE
Value	85.99	1.55	2.83
Value %	95.15 %	1.72 %	3.14 %
Uncertainty	7.762	1.735	2.549

Fig. 8: Sensitivity analysis for simulation Run 1, VAR = flaw depth, RATE = filling rate

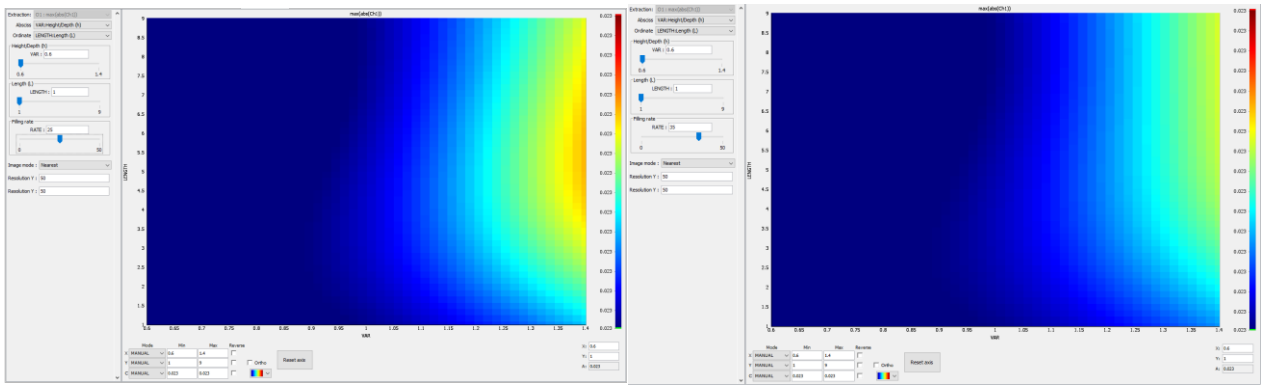

Fig. 9: Results of variation in notch depth, length, and notch filling rate parametric study. Map of maximum of absolute impedance plane amplitude. Notch filling rate = 25% for left image and notch filling rate = 35% for right image. VAR = flaw depth. Dimensions in mm

6. SIMULATION RUN 2 FOR VARIATION IN BACKWALL LIGAMENT AND FLAW LENGTH

Next, parameter 4 in section 4 is considered for simulation. Here, variation in ligament at a fixed a/t = 0.5 flaw is investigated. Ligament lengths from backwall are from 0 to 0.4 mm and flaw lengths are from 1 to 9 mm. The filling rate is 0 %. Current is 1 A. Rest of the parameters are same as in Run 1. Note that frequency is 175 kHz. Non-zero ligament flaw is described as embedded flaw. Embedded flaw is closer to the probe than backwall flaw. Therefore, signal response is likely to be higher. However, as eddy currents can flow through backwall ligament, and the eddy current response may dip slightly. Therefore, simulation may be useful in providing effect of change in backwall ligament on eddy current signal response.

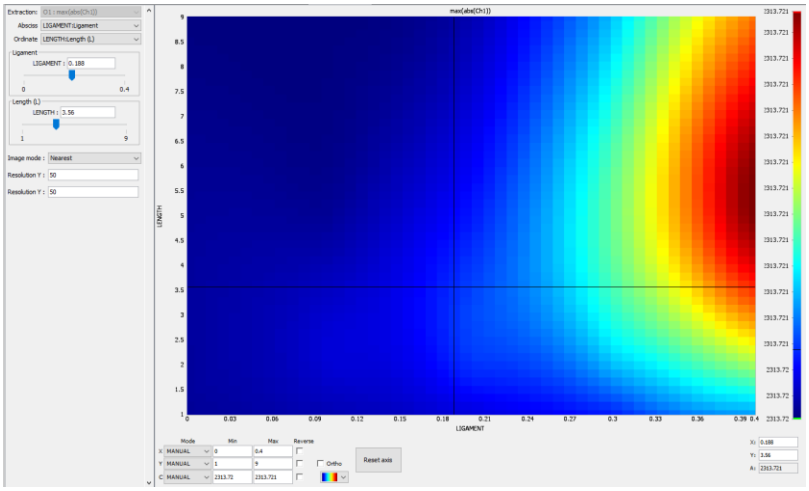

Fig. 10: Results of variation in ligament and length. Map of maximum of absolute impedance plane amplitude. Notch filling rate = 0 %. Frequency = 175 kHz.

Fig. 10 shows that as ligament from backwall increases, EC response increases. There seem to be a very slight dip in signal response for flaws longer than 5 mm. See top left corner of Fig. 10 graphic. DOP/t = 0.66 for Runs 1 and 2. A different distribution of amplitude is expected for higher values of DOP/t e.g., 1-2. Mostly, the signal response increases with increasing backwall ligament for a/t = 0.5 notch.

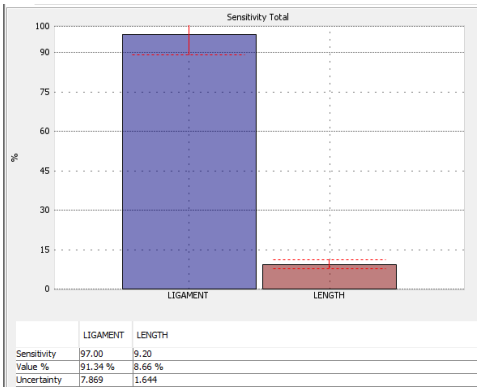

Fig. 11: Sensitivity Analysis for simulation Run 2

Sensitivity analysis in Fig. 11 indicates that the ligament is an order more sensitive than length.

7. SIMULATION RUN 3 FOR CHANGE IN FREQUENCY

Next frequency will be changed to study effect of change in frequency. Frequency of 75 kHz (DOP/t = 1.0) is chosen. Rest of the quantities are same as in Run 2.

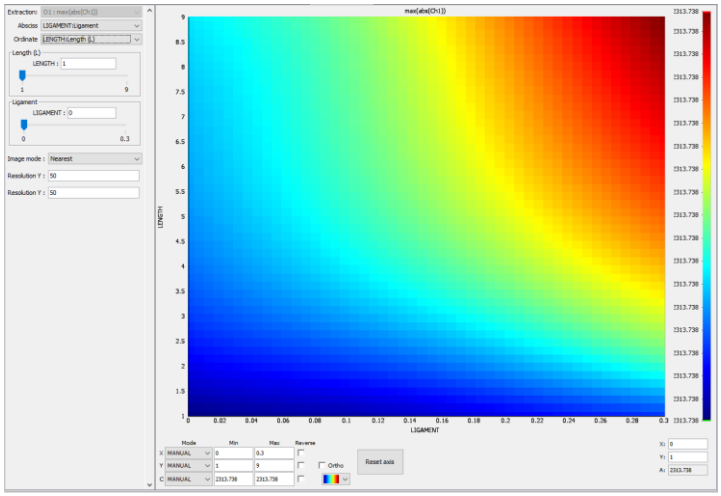

Fig. 12: Results of variation in ligament and length. Map of maximum of absolute impedance plane amplitude. Notch filling rate = 0 %. Frequency = 75 kHz.

Mostly, the signal response increases with increasing backwall ligament for a a/t = 0.5 notch. Therefore, between 75 kHz (DOP/t = 1.0) and 175 kHz (DOP/t = 0.66) the backwall a/t = 0.5 notch seems to provide lowest signal response and may provide worst-case signal response for T/R topology. Correlation between the backwall flaw response and identical embedded flaw response should be investigated by simulation, for coil topologies used in the inspection set-up. If there is difference in the backwall flaw response and worst-case embedded flaw response, an appropriate transfer function[13] may be used in the POD study.

8. SIMULATION RUN 4 FOR VARIATION IN FLAW SHAPE AND LENGTH

In this run, effect of differences between semi-elliptical and rectangular backwall notches is studied. Frequency is 175 kHz. Flaw size is given by a/t = 0.5. a = 1 mm.

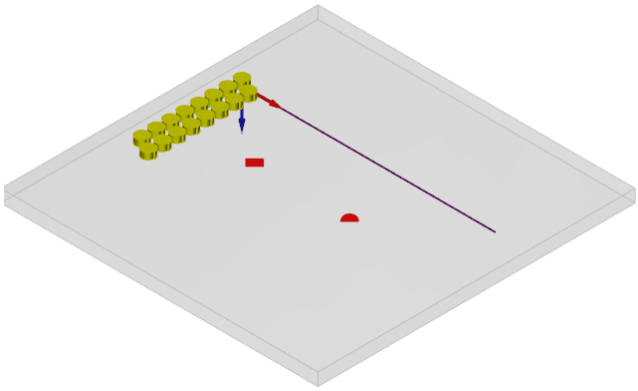

Fig. 13: Schematic of two backwall flaws with same depth and length dimensions. Left notch is rectangular and right notch is semi-elliptical.

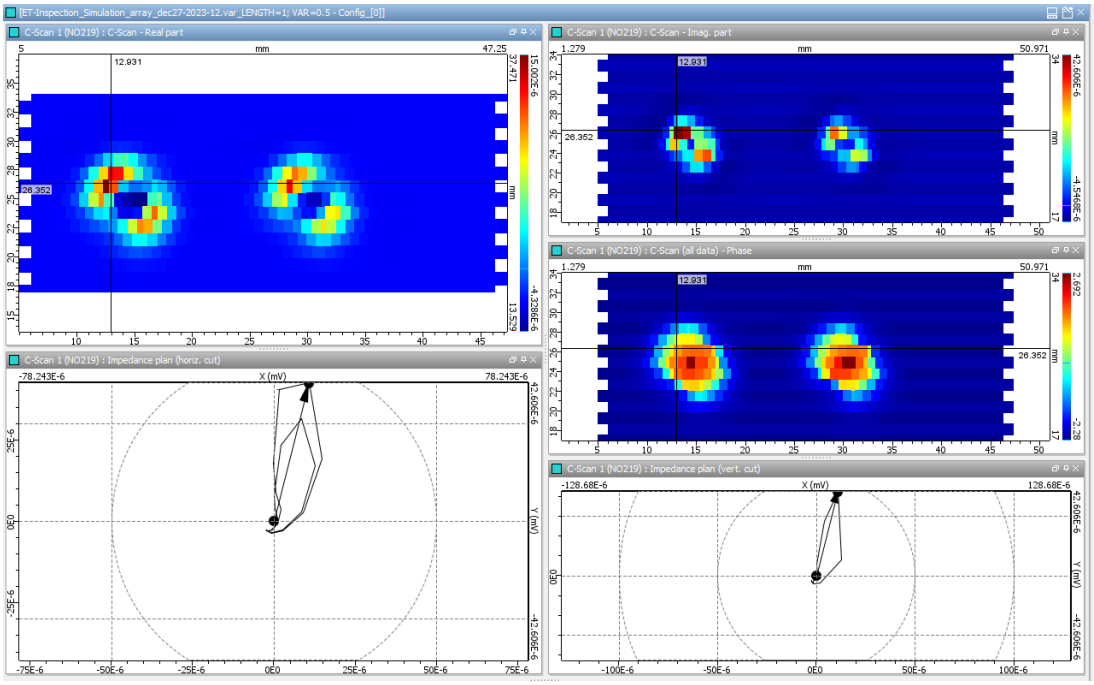

Fig. 14: Simulation data for *a*/*c* = 1 flaw. Left indication from rectangular notch and right indication from semi-elliptical notch

Rectangular notch indication registers ~ 40-50% higher vertical component of relative amplitude for real part compared to that of the semi-elliptical notch indication. Semi-elliptical flaw gives smaller size indication.

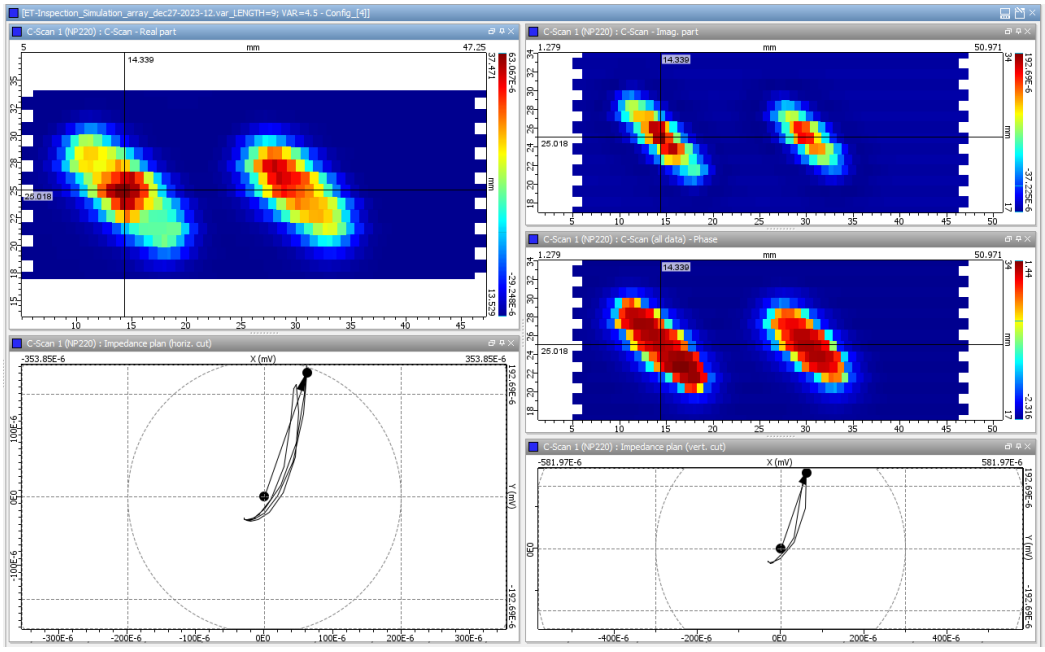

Fig. 15: Simulation data for *a*/*c* = 0.22 flaw. Left indication is from rectangular notch and right indication from semi-elliptical notch

Above observations are true for indications in Fig. 15. Based on above observations, it is recommended to use semi-elliptical surface notches in the calibration reference standard.

9. RUN 5 FOR VARIATION IN FLAW ORIENTATION

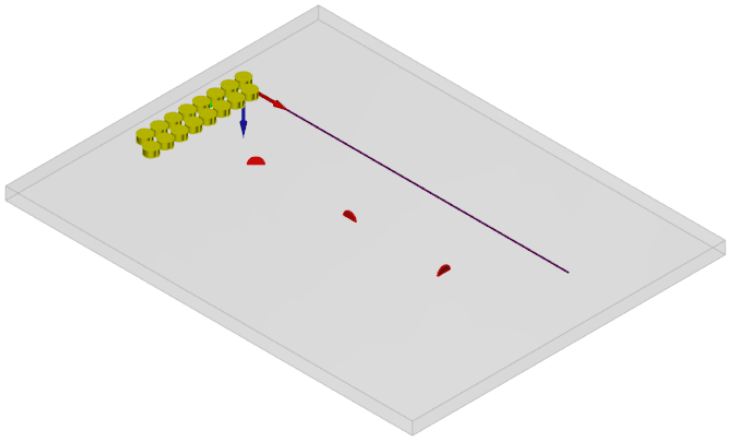

Fig. 16: Schematic of three backwall flaws with same depth and length dimensions, $a/c = 1$. From left to right orientations are: 45°, axial and transverse

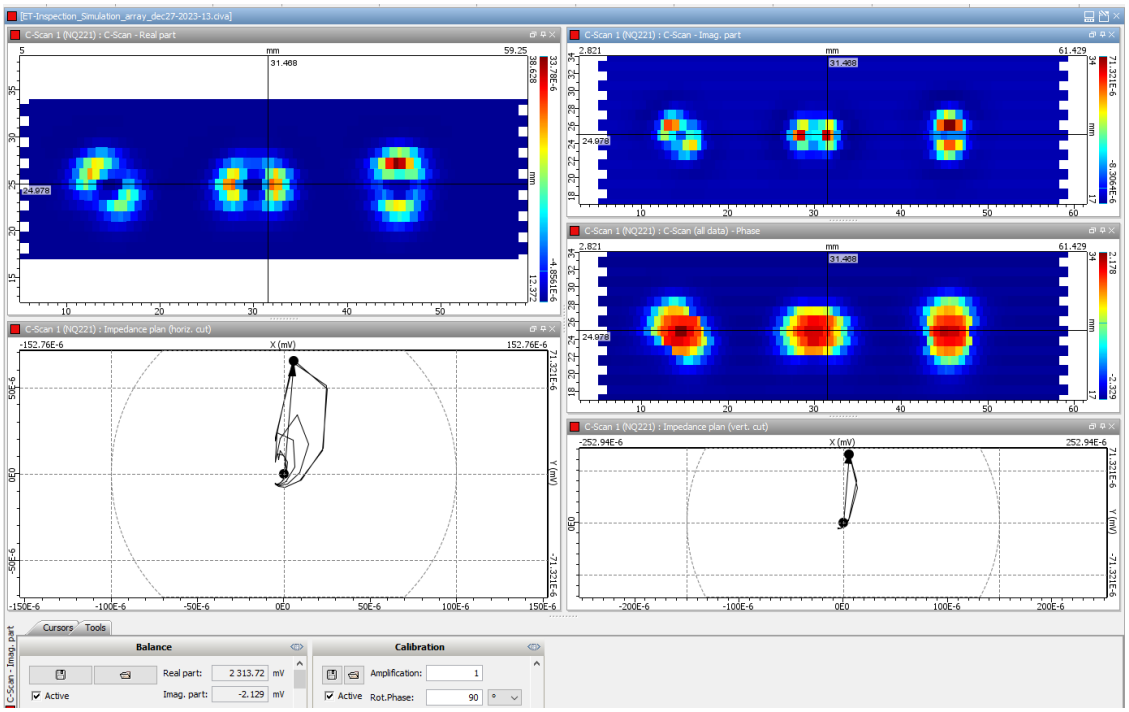

Fig. 17: Simulation results comparing indications from 45°, axial and transverse orientation flaws

Transverse flaw registered largest signal response (vertical component of real part) followed by axial flaw. 45° oriented flaw registered least signal response. 45° oriented flaw should be used in the reference standard.

10. RUN 6 FOR VARATION IN SIGNAL RESPONSE SENSITIVITY

Here, signal response sensitivity $S_{a/t}$ is defined as ratio of signal responses of backside EDM notch to same length through (the thickness) notch. Notch depth is the primary variable here. Sensitivity is a function of a/t. Higher ratio may be indicative of higher sensitivity. Very high frequencies will provide lower sensitivity. Higher sensitivity may imply better signal to noise ratio. Therefore, Sensitivity values are expected to be in certain range for reliable ECA techniques and would help in technique optimization.

$$S_{a/t} = \frac{y_a}{y_t} \tag{1}$$

$$S_{a,target/t} = \frac{y_{a,target}}{y_t} \tag{2}$$

where, y_a= maximum relative amplitude from flaw of depth "a",

y_t= maximum relative amplitude from through the thickness flaw, and

$y_{a,target}$ = maximum relative amplitude from target size flaw.

Run 1 input is used for length 2c = 2 mm flaw. Depth (a) values ranged from 0.1 to 2 mm in increments of 0.1 mm. Two frequency values are used. Plot of sensitivity function is provided in Fig. 18. It illustrates dependence of sensitivity on frequency.

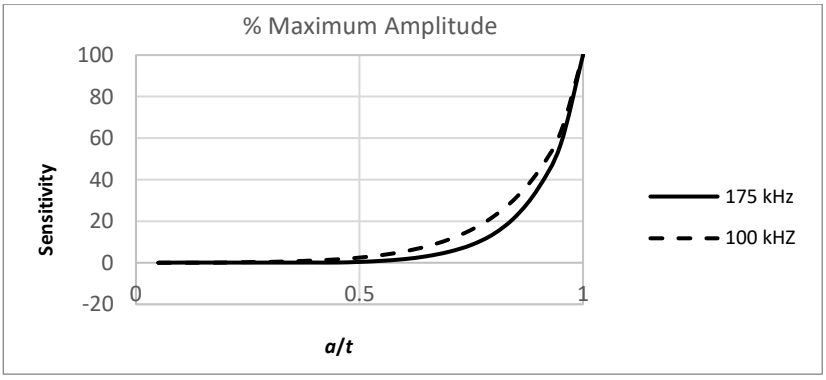

Fig. 18: Sensitivity function

Fig. 18, shows that for shallower flaws, signal response tends to be equal to zero. In practice it will be equal to noise. Thus, the largest ligament of artificial backwall flaw for a given length that can be barley imaged or distinguished from background, denoted as a_{noise}, can be used to define contrast sensitivity as follows,

$$c_s = \frac{a_{noise}}{t}. \tag{3}$$

Better contrast sensitivity (smaller value) is expected for detecting shallower flaws. Contrast sensitivity value shall be smaller than the $\frac{a_{target}}{t}$ else the target size natural flaws will not be detected. Upper limit on contrast sensitivity seems to be justified for a reliable ECA backwall flaw detection technique. Contrast sensitivity correlates with noise equivalent sensitivity. Better contrast sensitivity implies higher CNR.

11. ECA PROCEDURE CALIBRATION CONSIDERATIONS

Development of the ECA technique including calibration protocol is the first task of qualification. Calibration reference standard is used to set-up ECA technique to detect the target size crack on the backwall. 0° and 90° orientation flaws are of interest for fracture control. Therefore, these orientation flaws should be included in calibration reference standard. The 45° orientation flaw may be of lesser importance to fracture control. However, it provides least signal response among

three orientations. Therefore, it should be included in the calibration reference standard. The calibration sample should have 0°, 45°, and 90° orientation electro-discharge machined (EDM) flaws. EDM flaws are described as open flaws as there is no contact between the flaw face. The EDM flaws can be produced to tight tolerances for dimensions and root geometry. Other types of notches such as plasma focused ion beam (PFIB) notches and Laser machining notches may be comparable or better than EDM notches. EDM flaws have typically 0.004" opening. A fixed size opening ≤ 0.004" is preferred.

A nominal part configuration is assumed for calibration specimens. For example, consider an eddy current application of an orbital tube weld (OTW), the calibration specimen is an OTW specimen with exact material, wall thickness, diameter, and weld. The calibration flaw can be an EDM flaw on inner diameter (ID) with ID target size.

Some EDM flaws should be placed on the ID at the lowest point of root of weld and in transition region of weld root to HAZ. Additional flaws may be placed between the two locations. The EDM flaws are staggered circumferentially. The calibration flaw length and depth shall be same as the length and depth of the ID target flaw to be detected. Shape of the flaw should be semi-elliptical. Additional sub-target size flaws may be used if there is a need to assess flaw size margin to detect the target size flaw reliably. Sub-target flaws have the same length, but lower depth compared to the target flaw. Some through notches are also recommended. Relationship between signal response from the target and sub-target calibration flaws to that from a through notch of same length provides a measure of ECA technique sensitivity. Through notches have rectangular shape.

For example, dimensions of a qualification target size of surface semi-elliptical EDM flaw may be given as,
$a^{target} = 0.7t$, $2c^{target} = l^{target} = 0.1$", $w^{target} = 0.004$", $t = 0.080$",
where, a^{target} = target flaw depth,
$2c^{target} = l^{target}$ = target flaw length,
w^{target} = target size EDM flaw width, and
t = part thickness.
Sub-target size EDM flaw dimensions may be given as,
$a^{subtarget} = 0.6t$, $l^{subtarget} = 0.1$", $w^{subtarget} = 0.004$"

Table 1: Calibration reference standard notch descriptions

	Location				
	1	2	3	4	5
Orientation	**Root Center**	**Between Root Center and HAZ on Root Side**	**Root to HAZ Transition**	**Parent Material Near HAZ on Root Side**	**Parent Material Away from HAZ on Root Side**
Axial (0°)	-Target size notch -Target length through notch (optional)	-Target size notch (optional)	-Target size notch (optional)	-Target size notch -Target length through notch (optional)	-Long through notch*
Transverse (90°)	-Target size notch -Target length through notch (optional)	-Target size notch (optional)	-Target size notch (optional)	-Target size -Target length through notch (optional)	-Long through notch**
45°	-Target size notch -Sub-target notch (optional) -Target length through notch	-Target size notch (optional)	-Target size notch (optional)	-Target size notch -Sub-target size notch (optional) -Target length through notch	

*- longer than probe width
** - longer than probe length
Four weld root locations numbered 1 through 4 are used for notches. See Table 1. Location 5 is away from weld root. It is meant for verifying probe signal response uniformity on long flaws. Location 5 has long through notches. Three flaw orientations are included. Through (the thickness) EDM target length notches are included for 3 flaw orientations at 2 locations. Fig. 19 shows flaw locations in square blocks.

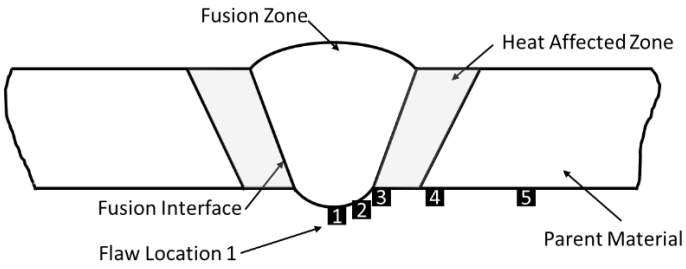

Fig. 19: Calibration flaw locations

Quantity for each notch in Table 1 is 1 each. Although replicates of the worst-case notch may be added as an option. Column 2 notches are optional, if their signal responses do not differ substantially from corresponding column 1 notches. Similarly, column 3 notches are optional if their signal responses do not differ substantially from corresponding column 4 notches. The lowest signal response from the target size notches is considered in setting up the ECA technique. Additional flaw locations may be chosen depending upon weld bead size relative to the target flaw size.

Sub-target notches may be used. Sub-target notches have target length but smaller depth. One sub-target size flaw is suggested in column 1 and 4 each of Table 1. More sub-target flaw sizes can be used to establish signal response (sensitivity) curve. Such curve may be useful in optimizing flaw detection by choice of probe, probe topology and frequency for a given application.

Noise can be measured as a standard deviation or peak value of irrelevant indications. If c-scan data is used in flaw detection, then contrast-to-noise ratio (CNR) may be measured. Standard deviation of noise is applicable for CNR measurement. If decision threshold is compared with the maximum amplitude of the flaw indication pixels, then peak signal noise is applicable.

Standard deviation of noise and peak noise can be measured from ECA scan of representative OTW for the chosen probe coil topologies. Standard deviation of noise is calculated in areas of indication background region of interest (ROI) areas where flaws are not present. Signal-to-noise (peak) ratio on calibration flaw should be measured. Noise equivalent EDM flaw depth or detection sensitivity can be estimated using the calibration curve of signal amplitude versus flaw depth for target flaw length. EDM flaw detection sensitivity measure can help in optimizing ECA technique. A calibration sample tube may be cut in two parts i.e., either in two halves or a window may be cut on opposite side to machine flaw on the tube ID. After EDM notch is machined, the two parts should be glued together to provide a smooth OD surface for probe movement.

12. EQUIVALENT EMBEDED FLAW SIZE

Embedded flaws will not be machined in calibration standards. The backwall semi-elliptical notch can be mapped in the elliptical embedded notch for ECA backwall flaw detection. If simulation indicates that the smallest embedded flaw response is not smaller than corresponding equal area, length, and depth semielliptical backwall notch, then following equivalency applies. Embedded flaw will have same depth and length and approximately same area as the backwall semi-elliptical flaw. See Table 2.

Table 2: mapping semi elliptical flaw shape to elliptical flaw shape

	Length	Depth
Semi-elliptical surface	$2c^s$	a^s
Elliptical embedded	$2c^e = 2c^s$	$2a^e = a^s$

If simulation indicates that smallest embedded flaw response is smaller than the corresponding equal area, length, and depth semielliptical backwall notch, then a transfer ratio of flaw lengths for semi-elliptical backwall and embedded worst-

case flaw providing same value of signal response may be determined using simulation and used to determine the equivalent embedded flaw size.

Tube curvature would have an effect of machining circumferential semi-elliptical flaw. The surface side of the flaw will be concave. The target circumferential machined flaw depth and area should be same as that required for the target flaw on flat surface. The mean of OD and ID arc lengths would be approximately same as that required for the target flaw on flat surface.

13. TRANSFER RATIO QUALIFICATION MODEL

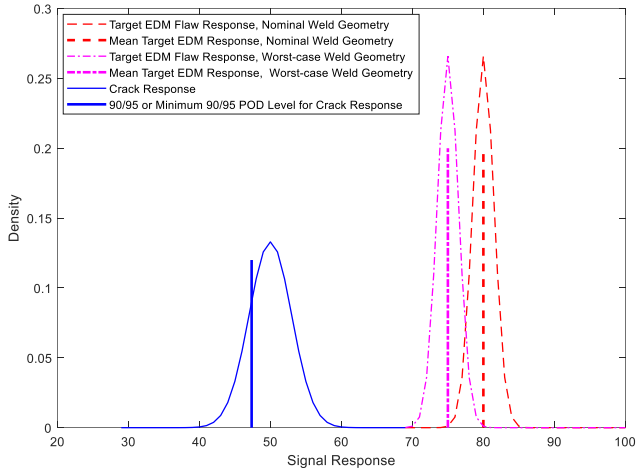

Fig. 20: Illustration of relative signal responses of EDM flaw in weld geometry specimens during qualification testing. Part crack response concept.

During qualification testing following transfer ratios should be estimated. First specimen set is made from simple geometry specimens. It has same target size semi-elliptical EDM notches and fatigue cracks. Crack-to-EDM signal response transfer ratio is given by,

$$R_{target,90/95}^{crack-EDM,simple\ geom} = \frac{y_{target,90/95}^{crack,simple\ geom}}{y_{target,mean}^{EDM,simple\ geom}}, \tag{4}$$

where, $R_{target,90/95}^{crack-EDM,simple\ geom}$ = crack-to-EDM signal response transfer ratio,

$y_{target,90/95}^{crack,simple\ geom}$ = fatigue crack signal response from simple geometry specimens, and

$y_{target,mean}^{EDM,simple\ geom}$ = EDM flaw signal response from simple geometry specimens.

Sample size of minimum 3 is recommended for $y_{target,mean}^{EDM,simple\ geom}$ estimation. Sample size of minimum 7-10 is recommended for $y_{target,90/95}^{crack,simple\ geom}$ estimation. Second specimen set is made from part geometry specimens with two cases. Half specimens have nominal part (e.g., weld) geometry and the half specimens have worst part geometry. Worst part geometry to nominal part geometry signal response transfer ratio is given by,

$$R_{target}^{worst-nominal\ part\ geom} = \frac{y_{target,mean}^{EDM,worst\ part}}{y_{target,mean}^{EDM,nominal\ part}} \tag{5}$$

$R_{target}^{worst-nominal\ part\ geom}$ = worst to nominal part geometry signal response transfer ratio,

$y_{target,mean}^{EDM,worst\ part}$= worst-case part geometry, and

$y_{target,mean}^{EDM,nominal\ part}$ = nominal part geometry signal response.

Sample size of minimum 3 each are recommended for $y_{target,mean}^{EDM,worst\ part}$ and $y_{target,mean}^{EDM,nominal\ part}$ estimations. Above geometry transfer ratio may be ignored if it is approximately equal to 1. Crack-to-EDM flaw transfer ratio is computed by following equation.

$$R_{target,90/95}^{crack/EDM} = R_{target,90/95}^{crack-EDM,simple\ geom} \times R_{target}^{worst-nominal\ part\ geom}, \tag{6}$$

where, $R_{target,90/95}^{EDM/crack}$ = transfer ratio of mean target size EDM flaw signal response to same size worst-case target crack in simple geometry specimens. The bounding signal response form crack in part can be estimated as,

$$y_{target,90/95}^{crack,part} \cong R_{target,90/95}^{crack/EDM} \times y_{target,mean}^{EDM,nominal\ part} \tag{7}$$

where, $y_{target,90/95}^{crack,part}$= estimated 90/95 Probability/Conf. signal response from target size crack, and

$y_{target,mean}^{EDM,nominal\ part}$ = mean target size calibration EDM flaw signal response. See Fig. 20 for rightmost thick vertical dashed line.

In practice, $R_{target,90/95}^{crack/EDM}$ may not be known exactly for a given ECA technique. Qualification testing on many inspection cases may indicate a lower minimum POD/Conf. 90/95% bound denoted as $y_{target,90/95\min}^{worst\ crack,part}$, with constraints on the ECA technique as supported by the qualification testing data. The constraints may be for ECA technique parameters including flaw-material characteristics. Upper limit for decision threshold is calculated from calibration flaw response as follows.

$$y_{target,90/95\min}^{crack,part} \leq R_{target,90/95\min}^{crack/EDM} \times y_{target,mean}^{EDM,nominal\ part}, \tag{8}$$

where, $y_{target,90/95\min}^{crack,part}$= estimated minimum 90/95 POD/Conf. signal response from target size crack.

In Fig. 21, crack response distribution is not shown. Only predicted lower limit for minimum 90/95 POD crack response is indicated by a thick solid vertical line.

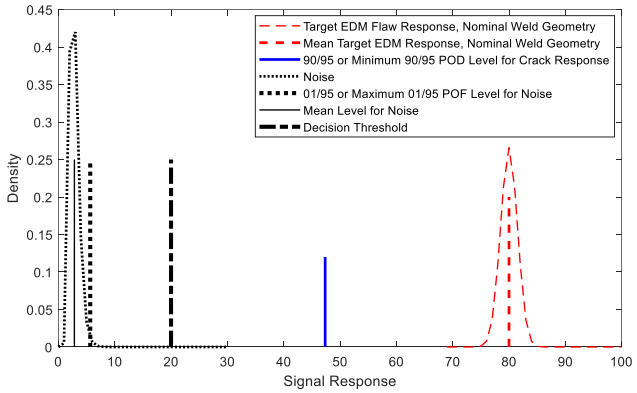

Fig. 21: Illustration of relative signal responses of EDM flaw, and noise, in part geometry specimens.

The worst-case geometry specimens are also used to measure noise and define noise distribution. Fig. 21 also shows noise distribution on worst-case qualification part configuration specimens. The 01/95% POF/Conf. equivalent noise is denoted as $y_{POF,01/95}^{noise,qual}$. Noise is also measured on part during actual inspection.

Following inequality is desired for applicability of qualification testing,

$$y_{POF,01/95}^{noise,part} \leq y_{POF,01/95}^{noise,qual}, \tag{9}$$

where, $y_{POF,01/95}^{noise,part}$ = 01/95 POF/Conf. equivalent noise on part. See Fig. 21 thick vertical dotted line.

Qualification testing on many inspection cases may indicate an upper bound maximum 1% POF noise denoted by $y_{POF,01/95\max}^{noise,qual}$ with constraints on the ECA technique as supported by the qualification testing data. This is expressed as,

$$y_{POF,01/95}^{noise,part} \leq y_{POF,01/95\max}^{noise,qual}, \tag{10}$$

where, $y_{POF,01/95\max}^{noise,part}$ = maximum 01/95 POF/Conf. equivalent noise on part. See Fig. 21 thick vertical dotted line.

Following inequality should be met during qualification,

$$y_{POF,01/95\max}^{noise,qual} \leq y_{thr} \leq y_{target,90/95\min}^{worst\ crack,part}. \tag{11}$$

Following inequality should be verified for each ECA technique to ensure reliable flaw detection.

$$y_{POF,01/95}^{noise,part} \leq y_{thr} \leq y_{target,90/95\min}^{worst\ crack,part}, \tag{12}$$

y_{thr} = decision threshold. See Fig. 21 thick vertical dash-dot line.

Net signal response and net decision threshold are measured over mean noise level which is shown as a thin vertical solid line in the middle of noise distribution. Noise should be measured on the inspection part too. Noise analysis may use different distributions such as normal or lognormal. 1% POF net threshold to noise (standard deviation) ratio (TNR) value should be greater than or equal to ~2.3 for noise modeled as normal distribution and ~3.7 for noise modeled as lognormal distribution. Calibration of ECA technique and with noise measured on the part and meeting Eq. (11) condition verifies the technique reliability.

14. ECA TRANSFER RATIO QUALIFICATION

Second task of ECA qualification testing is to estimate EDM flaw to crack signal response transfer ratio as defined Eq. (4A) and Eq. (5). Previous section explains the transfer ratio model. Development ECA procedure and estimation of transfer ratio are necessary steps in ECA qualification. It is assumed that the EDM flaws can be manufactured to close tolerances. It is assumed that the fatigue cracks can be manufactured to fracture control requirements and have predictable $a/2c$. $a/2c$ may be function of the crack surface length. Fatigue cracks are considered to be the worst-case in terms of crack tightness or contact/gap between faces. Other factors to consider in empirical study for transfer ratio estimation are:

- Specimen geometry: Simple geometry, nominal and worst-case part geometry specimens
- Material: For example, selected aluminum alloy, titanium alloy stainless steel, Inconel
- Flaw orientation: 0, 45, 90°
- Flaw depth: Variation in a/t ratio
- Instrument, probe type, topology, frequency, set-up details (step/index, filter setting), similarity of probes for simple geometry and part geometry
- DOP/part thickness ratio
- Standard depth of penetration (DOP)/ligament ratio
- Flaw length to resolution ratio $2c/r$

Well defined calibrated techniques should be used to gather qualification data. Decision threshold is not needed for gathering transfer ratio qualification data. Bounding cases in terms of (DOP)/part thickness and (DOP)/ligament, ligament/probe resolution and flaw length/resolution should be considered.

Standard NDE requires POD testing of group of qualified operators[8] in determining reliably detectable flaw size. Simple geometry fatigue crack specimens are needed to conduct operator POD testing for both Standard and Special eddy current applications. An empirical forward transfer function[11-13] study is needed to determine demonstration size cracks. The POD demonstration fatigue crack sets in simpler geometry specimens should be manufactured.

It would be advisable to design experiments to cover all combinations of material-flaw characteristics, instrumentation in the qualification. Qualification data analysis should provide bounding values of transfer ratio with constraints on flaw, material, set-up etc. If testing is conducted in phases, initial phases may define objectives of later phases and may save cost and time.

15. ECA QUALIFICATION TAKS

Based on previous discussion a list of ECA qualification is suggested.

1. Develop ECA calibration reference standard design in part geometry/material specimen
    a. Use target size flaws (Sec. 11)
    b. Fabricate reference standards
2. Develop ECA procedures
    a. Define qualified flaw size and constraints
    b. Calibration on reference standard
    c. Sensitivity measurement on reference standard, technique optimization (Sec. 10)
    d. Noise measurement on part (Sec. 4, 11)
3. Transfer ratio qualification (Sec. 13, 14)
    a. Empirical testing, bounding cases of DOP ratios DOP/t, DOP/d_l and resolution ratio $2c/r$, where $d_l =$ ligament of backwall target size flaw, and r = ECA probe resolution in the chosen topology. Bounding values are lowest among the techniques
    b. Cover every type of probe and topology used in the ECA procedures
    c. Cover frequencies that are considered to be less than optimal for chosen probe
    d. Create a database that can be sorted based on set-up input parameters, DOP ratios, and resolution ratios. Database should provide references to test reports. See appendix A
    e. Document of ECA set-ups and transfer ratio analysis
    f. Provide guidelines to use the transfer ratio data documentation
    g. Provide reference to the guidelines document in the ECA procedure
4. Update ECA procedures
    a. Verify that estimated target flaw signal response and TNR can be calculated and conditions on these parameters can be implemented (Sec. 13)
5. Forward transfer function study
    a. Perform transfer function study[11,12,13] for determining demonstration flaw size in simple geometry specimens
    b. ECA technique developer to perform non-blind POD testing to assess degree of difficulty in passing blind POD demonstration test
    c. Optimize ECA techniques and update ECA procedure
6. POD demonstration tests (Standard or Special)
    a. Perform blind POD demonstration tests
    b. POD data analysis, qualification/certification report

16. CONCLUSION

This paper uses simulation to investigate essential parameters in ECA testing in detection of backwall and embedded cracklike flaws. Based on simulation results, choice of calibration reference standard design, transfer ratio qualification model is suggested. The paper points to many considerations for ECA technique qualification. Tasks for completing the qualification study are listed. These considerations are also applicable to single sensor EC testing.

17. ACKNOWLEDGEMENTS

David Stanley, Nathan Trepal, and Samik Das provided technical review and valuable suggestions to this paper.

REFERENCES

1. Eddyfi Technologies, https://www.eddyfi.com/
2. Zetec, https://www.zetec.com/products/eddy-current/
3. Evident, https://www.evidentscientific.com/, https://www.olympus-ims.com/
4. SG NDT, https://sgndt.com/
5. Uniwest, https://www.uniwest.com/
6. NASGRO® FRACTURE MECHANICS & FATIGUE CRACK GROWTH SOFTWARE, https://www.swri.org/consortia/nasgro
7. Bishop, C. R. (1973): "Nondestructive Evaluation of Fatigue Cracks," Space Division Rockwell International, SD 73-SH-0219, NASA Contractor Report NAS9-14000, 1973.
8. Parker Peter, Forsyth David, Suits, Michael, Walker James, Koshti Ajay and Prosser, William., "Guidebook for the Design and Analysis of a customer Standard Nondestructive Evaluation (NDE) Probability of Detection (POD) Study," NESC-TI-21-01657, customer STI, https://www.sti.customer.gov/, https://ntrs.customer.gov/, NASA Langley Research Center, (2022).
9. EXTENDE CIVA NDT Simulation Software, extende.com
10. Koshti Ajay, Parker Peter, Forsyth David, Suits, Michael, Walker James, and Prosser, William, "Guidebook for Limited Sample Probability of Detection (LS-POD) Demonstration for Single Hit Nondestructive Evaluation (NDE) Methods," NASA Langley Research Center, NESC-TI-20-01545, (2021).
11. Koshti Ajay, Parker Peter, Forsyth David, Suits, Michael, Walker James, and Prosser, William, "Guidebook for Assessing Similarity and Implementing Empirical Transfer Functions for Probability of Detection (POD) Demonstrations for Single-Hit Nondestructive Evaluation (NDE) Methods", NASA Langley Research Center, (2022).
12. Koshti Ajay M., "Transfer function models and sensitivity analysis," SPIE Smart Structures and NDE, SPIE 12488, (2023).
13. Koshti A.M. "Transfer function models for using empirical and physics-based simulation signal response data," SPIE Smart Structures and NDE, (2024).
14. Koshti, Ajay M., "Optimizing raster scanning parameters in nondestructive evaluation using simulation of probe sensitivity field," SPIE Smart Structures and NDE, Proc. SPIE 11592, (2021).
15. Koshti, Ajay M., "Assessing Visual and System Flaw Detectability in Nondestructive Evaluation," SPIE Smart Structures and NDE, SPIE 11592, (2021).

Appendix A

Table A1: Example of suggested database fields for weld crack-to-EDM transfer ratio data

Set-up No.	Specimen: Geometry type	Tube Diameter, mm	Height or Part thickness, mm	Material	Electrical Conductivity, MSm^{-1}	Relative Magnetic Permeability	Probe Specification	Topology	Flaw position	Flaw description	Nominal length 2c, mm	Nominal depth, a, mm	Artificial flaw	Sample size for artificial flaw	Set 1	Set 1 ID	Sample size for set 1	Set 2	Set 2 ID	Sample size for set 2	Flaw orientation, deg.	Frequency, kHz	Coil spacing, mm	Row offset, mm	Scanning Step, mm	Expected probe resolution, r, mm	Flaw Ligament, d_l, mm	DOP/t	DOP/d_l	2c/r	$R^{worst-nominal\ part\ geom}_{target}$	Set-up file name	Report No.
1	Welded tube	6.4	2	Stainless Steel 304L	0.8	1	X	SDDA	backwall	Semi-elliptical	2	1	EDM	3	Nominal weld topography	XX	3	Worst case weld topography	XXX	3	0	175	2.3	1.3	1	1.3	1	0.7	1.3	2	0.9	XX XX	XXXX X
1	Welded tube	6.4	2	Stainless Steel 304L	0.8	1	X	SDDA	backwall	Semi-elliptical	2	1	EDM	3	Nominal weld topography	XX	3	Worst case weld topography	XXX	3	90	175	2.3	1.3	1	1.3	1	0.7	1.3	2	0.9	XX XX	XXXX X
1	Welded tube	6.4	2	Stainless Steel 304L	0.8	1	X	SDDA	backwall	Semi-elliptical	2	1	EDM	3	Nominal weld topography	XX	3	Worst case weld topography	XXX	3	45	175	2.3	1.3	1	1.3	1	0.7	1.3	2	0.9	XX XX	XXXX X
1	Welded tube	6.4	2	Stainless Steel 304L	0.8	1	X	SDDT	backwall	Semi-elliptical	2	1	EDM	3	Nominal weld topography	XX	3	Worst case weld topography	XXX	3	90	175	2.3	1.3	1	1.3	1	0.7	1.3	2	0.9	XX XX	XXXX X
1	Welded tube	6.4	2	Stainless Steel 304L	0.8	1	X	SDDT	backwall	Semi-elliptical	2	1	EDM	3	Nominal weld topography	XX	3	Worst case weld topography	XXX	3	##	175	2.3	1.3	1	1.3	1	0.7	1.3	2	0.9	XX XX	XXXX X
1	Welded tube	6.4	2	Stainless Steel 304L	0.8	1	X	SDDT	backwall	Semi-elliptical	2	1	EDM	3	Nominal weld topography	XX	3	Worst case weld topography	XXX	3	##	175	2.3	1.3	1	1.3	1	0.7	1.3	2	0.9	XX XX	XXXX X

Table A2: Example of suggested database fields for weld geometry transfer function data

Set-up No.	Specimen: Geometry typ	Tube Diameter, mi	Height or Part thickness, mm	Material	Electrical Conductivity, MSm^{-1}	Relative Magnetic Permeability	Probe Specification	Topology	Flaw position	Flaw description	Nominal length 2c, mm	Nominal depth, a, mm	Artificial flaw	Sample size for artificial flaw	Set 1	Set 1 ID	Sample size for set 1	Set 2	Set 2 ID	Sample size for set 2	Flaw orientation, deg.	Frequency, kHz	Coil spacing, mm	Row offset, mm	Scanning Step, mm	Expected probe resolution, r, mm	Flaw Ligament, d_l, mm	DOP/t	DOP/d_l	2c/r	$R_{worst-nominal\ part\ geom\ target}$	Set-up file name	Report No.
1	Welded tube	6.4	2	Stainless Steel 304L	0.8	1	X	SDDA	backwall	Semi-elliptical	2	1	EDM	3	Nominal weld topography	XX	3	Worst case weld topography	XXX	3	0	175	2.3	1.3	1	1.3	1	0.7	1.3	2	0.9	XXXX	XXXX
1	Welded tube	6.4	2	Stainless Steel 304L	0.8	1	X	SDDA	backwall	Semi-elliptical	2	1	EDM	3	Nominal weld topography	XX	3	Worst case weld topography	XXX	3	90	175	2.3	1.3	1	1.3	1	0.7	1.3	2	0.9	XXXX	XXXX
1	Welded tube	6.4	2	Stainless Steel 304L	0.8	1	X	SDDA	backwall	Semi-elliptical	2	1	EDM	3	Nominal weld topography	XX	3	Worst case weld topography	XXX	3	45	175	2.3	1.3	1	1.3	1	0.7	1.3	2	0.9	XXXX	XXXX
1	Welded tube	6.4	2	Stainless Steel 304L	0.8	1	X	SDDA	backwall	Semi-elliptical	2	1	EDM	3	Nominal weld topography	XX	3	Worst case weld topography	XXX	3	90	175	2.3	1.3	1	1.3	1	0.7	1.3	2	0.9	XXXX	XXXX
1	Welded tube	6.4	2	Stainless Steel 304L	0.8	1	X	SDDA	backwall	Semi-elliptical	2	1	EDM	3	Nominal weld topography	XX	3	Worst case weld topography	XXX	3	##	175	2.3	1.3	1	1.3	1	0.7	1.3	2	0.9	XXXX	XXXX
1	Welded tube	6.4	2	Stainless Steel 304L	0.8	1	X	SDDA	backwall	Semi-elliptical	2	1	EDM	3	Nominal weld topography	XX	3	Worst case weld topography	XXX	3	##	175	2.3	1.3	1	1.3	1	0.7	1.3	2	0.9	XXXX	XXXX